Probing lepton flavor violation signal via $e^+e^-(\gamma\gamma) \to l_i\bar{l}_j$ in the littlest Higgs model with T-parity at the ILC

Jinzhong Han, Xuelei Wang,* and Bingfang Yang

College of Physics and Information Engineering,

Henan Normal University, Xinxiang 453007, China

Abstract

In the littlest Higgs model with T-parity, the new interactions between the mirror leptons and the Standard Model leptons can induce some lepton flavor violation (LFV) processes at loop level. We study the possibility of the ILC to probe the LFV production processes $e^+e^-(\gamma\gamma) \to l_i\bar{l}_j$. Our results show that the rates of $\gamma\gamma \to l_i\bar{l}_j$ can reach 1 fb in optimal cases after reasonable kinematical cuts, which implies that these processes may be observed at the ILC.

PACS numbers: 14.60.-z,12.60.-i, 12.15.Mn,13.66.De

*Electronic address: wangxuelei@sina.com

I. INTRODUCTION

The little Higgs theory is proposed as an elegant solution to the hierarchy problem of the Standard Model (SM) and is now an important candidate of new physics [1]. Among various little Higgs models, the Littlest Higgs (LH) model [2] is the simplest but phenomenologically viable model, which incorporates all essential ingredients of the little Higgs theory. Unfortunately, this economic model suffers from severe constraints from the precisely measured electroweak data, and one has to tune finely its parameters to survive the constraints [3]. To avoid this problem, a new discrete symmetry called T-parity was introduced and the resulting model is referred to as the Littlest Higgs model with T-parity (LHT) [4]. In the LHT model, all dangerous contributions to the electroweak data are loop suppressed, and consequently wide regions of its parameter space are consistent with the data even when the breaking scale of the T-parity, f, is as low as 500 GeV [5]. On the other hand, to implement the T-parity one has to introduce a mirror fermion (T-odd quark/lepton) for each SM fermion. In general, the mass matrix for the mirror quarks/leptons is not proportional to that of their SM counterparts, and due to the misalignment of the mass matrix, neutral flavor changing (FC) interactions between the two types of fermions may naturally appear, which will induce flavor changing neutral current (FCNC) processes for both quarks and leptons at loop level [6–9]. Since these processes are highly suppressed in the SM, they can be utilized to probe new physics and any observation of them will undoubtedly imply the existence of new physics.

Since the observation of the neutrino oscillation, searching for the LFV signals at colliders has attracted more and more attention [10–13]. The LFV production processes, such as $pp(\bar{p}) \to l_i\bar{l}_j$ [14] and $\gamma\gamma \to l_i\bar{l}_j$, have been studied in R-parity conversing MSSM [14, 15], R-parity violating MSSM [16] and TC2 model [17]. These study indicates that the production rates can be several order larger than those in the SM and may reach the sensitivity of future experiments. We note that, in the LHT the FC interaction can also induce the production processes, and compared the LFV decays such as $l_i \to l_j\gamma$, $l_i \to l_j l_k l_l$, $\tau \to \mu\pi$ studied in the LHT model [18–20] with the decays in other new physics models [15, 16], we infer that the production rate is not suppressed in comparison with the predictions of the other model. This encourages us to study the production processes in detail. Among different production processes, we are more interested in $e^+e^-(\gamma\gamma) \to l_i\bar{l}_j$

($i \neq j$ and $l_i = e, \mu, \tau$) occurred at the proposed International Linear Collider (ILC) since the ILC provides rather clean environment to probe these processes.

This paper is organized as follows. In Section II we briefly review the LHT model. In Section III and IV, we show the details of our calculation of the production rates and present numerical results respectively. Finally, a short conclusion is drawn in Section V.

II. REVIEW OF THE LHT MODEL

In this sector, we briefly recapitulate the structure of the LHT model and define the conventions of our notation. A detailed description of the model can be found in [6, 7].

Basically speaking, the LHT model is a non-linear sigma model describing the spontaneous breaking of a global $SU(5)$ down to a global $SO(5)$. This symmetry breaking takes place at the scale $f \sim \mathcal{O}$ (TeV), and along with this breaking, there arise 14 Goldstone bosons which are described by the "pion"matrix

$$\Pi = \begin{pmatrix} -\frac{\omega^0}{2} - \frac{\eta}{\sqrt{20}} & -\frac{\omega^+}{\sqrt{2}} & -i\frac{\pi^+}{\sqrt{2}} & -i\phi^{++} & -i\frac{\phi^+}{\sqrt{2}} \\ -\frac{\omega^-}{\sqrt{2}} & \frac{\omega^0}{2} - \frac{\eta}{\sqrt{20}} & \frac{v+h+i\pi^0}{2} & -i\frac{\phi^+}{\sqrt{2}} & \frac{-i\phi^0+\phi^P}{\sqrt{2}} \\ i\frac{\pi^-}{\sqrt{2}} & \frac{v+h-i\pi^0}{2} & \sqrt{4/5}\eta & -i\frac{\pi^+}{\sqrt{2}} & \frac{v+h+i\pi^0}{2} \\ i\phi^{--} & i\frac{\phi^-}{\sqrt{2}} & i\frac{\pi^-}{\sqrt{2}} & -\frac{\omega^0}{2} - \frac{\eta}{\sqrt{20}} & -\frac{\omega^-}{\sqrt{2}} \\ i\frac{\phi^-}{\sqrt{2}} & \frac{i\phi^0+\phi^P}{\sqrt{2}} & \frac{v+h-i\pi^0}{2} & -\frac{\omega^+}{\sqrt{2}} & \frac{\omega^0}{2} - \frac{\eta}{\sqrt{20}} \end{pmatrix}. \tag{1}$$

Among the Goldstone bosons, the fields $\omega^0, \omega^\pm$ and η are eaten by the new T-odd heavy gauge bosons Z_H, $W_H^\pm$ and A_H. As a result, these gauge bosons acquire masses which up to $\mathcal{O}(v^2/f^2)$ are given by

$$M_{W_H^\pm} = M_{Z_H} = gf(1 - \frac{v^2}{8f^2}), \qquad M_{A_H} = \frac{g'}{\sqrt{5}} f(1 - \frac{5v^2}{8f^2}) \tag{2}$$

with g and g' denoting the SM $SU(2)$ and $U(1)$ gauge couplings respectively and v being the electroweak breaking scale. Quite similarly, the fields π^0 and $\pi^\pm$ are eaten by the SM gauge bosons (T-even) after the electroweak symmetry breaking. The masses of the Z and W bosons are then given by

$$M_{W_L} = \frac{gv}{2}(1 - \frac{v^2}{12f^2}), \qquad M_{Z_L} = \frac{gv}{2\cos\theta_W}(1 - \frac{5v^2}{12f^2}). \tag{3}$$

Note in the LHT model, the neutral gauge boson A_H is the lightest T-odd particle, and due to the conservation of T-parity, it is stable and thus can act as an dark matter candidate [5].

In order to implement the T-parity, each SM fermion must be accompanied by its mirror fermion. The particle content of the LHT then includes the T-even fermions, such as the SM quarks, leptons and an additional heavy quark T_+, and their mirror fermions. In this paper, we denote the mirror leptons by

$$\begin{pmatrix} l_H^1 \\ \nu_H^1 \end{pmatrix}, \quad \begin{pmatrix} l_H^2 \\ \nu_H^2 \end{pmatrix}, \quad \begin{pmatrix} l_H^3 \\ \nu_H^3 \end{pmatrix}. \tag{4}$$

with their masses given by [6, 7]

$$m_{l_H^i} = \sqrt{2}\kappa_i f \equiv m_{H_i}, \quad m_{\nu_H^i} = m_{H_i}(1 - \frac{v^2}{8f^2}) \tag{5}$$

Obviously, neglecting the $\mathcal{O}(v^2/f^2)$ correction to $m_{\nu_H^i}$ (i is generation index), the mirror neutrino and the mirror lepton in the same generation are degenerated in mass.

In a similar way to what happens for the SM fermions, the mirror sector has weak mixing parameterized by unitary mixing matrices, i.e. V_{H_l}, V_{H_ν} for mirror leptons and V_{H_u}, V_{H_d} for mirror quarks which satisfy the following physical constraints:

$$V_{H_\nu}^\dagger V_{H_l} = V_{PMNS}, \quad V_{H_u}^\dagger V_{H_d} = V_{CKM}. \tag{6}$$

These mirror mixing matrices imply flavor violating interactions between SM fermions and mirror fermions that are mediated by the heavy gauge boson W_H, Z_H and A_H. The relevant Feynman rules are given in [8].

III. CALCULATIONS

A. The LFV interaction $\bar{l}_i l_j V (V = \gamma, Z)$ in the LHT model

We have mentioned that the interaction between the mirror lepton and the SM lepton, such as $\bar{l}_H l Z_H(A_H)$ and $\bar{\nu}_H l W_H$, can induce LFV interactions at loop level. The relevant Feynman diagrams are shown in Fig. 1 for $\bar{l}_i l_j Z$ and $\bar{l}_i l_j \gamma$ vertexes. Unlike the previous studies where the unitary gauge were used in the calculation [18, 19], we use Feynman

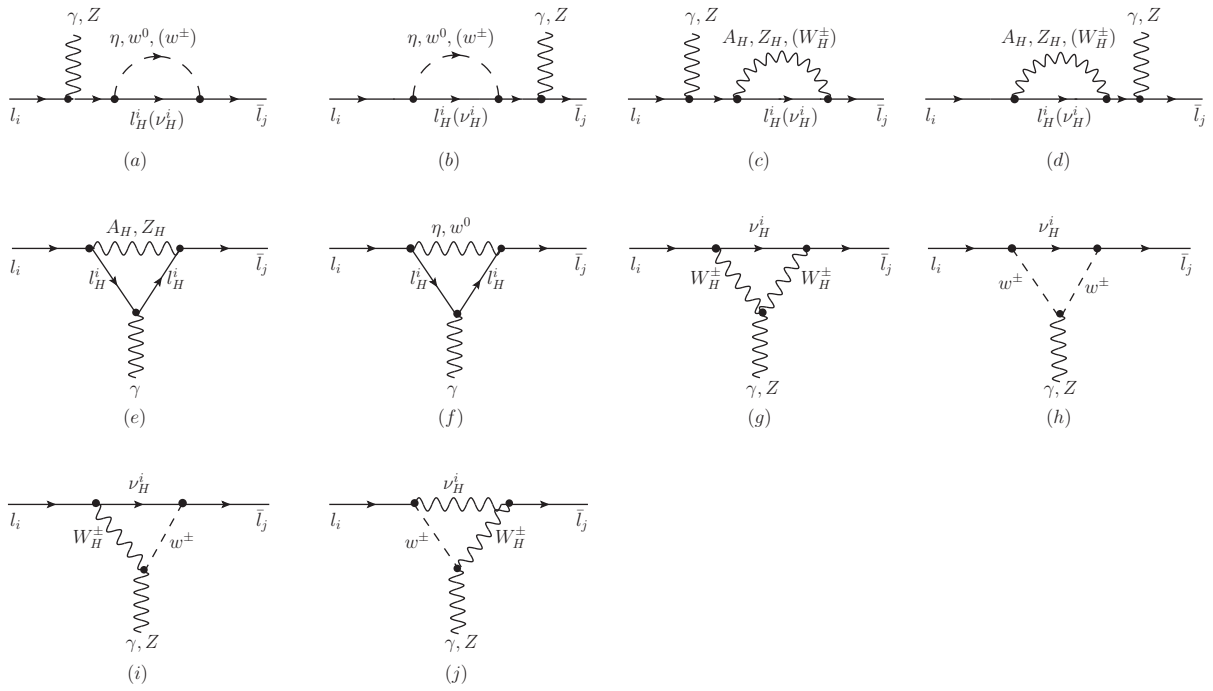

FIG. 1: Feynman diagrams contributing to the LFV vertex $l_i\bar{l}_j Z(\gamma)$ in the LHT model.

gauge to obtain our results, and that is why we also plot the diagrams involving the Goldstone bosons η, ω^0 and $\omega^\pm$ in Fig. 1. We once compared our results for the decay $l_i \to l_j\gamma$ with [19] and found we can reproduce Fig. 4 of this literature. Note in the LHT, the T-odd scalar triplet Φ in Eq. (1) can also contribute to the LFV vertex by the $\bar{l}_H l\Phi$ interaction. However, since such interaction is suppressed by v^2/f^2, we can neglect its contribution at the leading order of v/f expansion.

The Feynman diagrams for the production $e^+e^-(\gamma\gamma) \to l_i\bar{l}_j$ are shown in Fig. 2 with the black square denoting the loop-induced $\bar{l}_i l_j Z(\gamma)$ vertex. One important difference of the $\bar{l}_i l_j\gamma$ vertex in $e^+e^- \to l_i\bar{l}_j$ and in $\gamma\gamma \to l_i\bar{l}_j$ is both the leptons are on-shell for $e^+e^- \to l_i\bar{l}_j$, while either l_i or l_j is off-shell for $\gamma\gamma \to l_i\bar{l}_j$. In order to simplify calculation, we'd better use an universal form of the $\bar{l}_i l_j\gamma$ vertex which is valid for the both cases. This is possible as suggested by [21]. In our calculation, we use the method in [21] to get the effective $\bar{l}_i l_j Z(\gamma)$ vertex and present their expressions in detail in Appendix A. We numerically check the rates of the production processes are free of ultraviolet divergence.

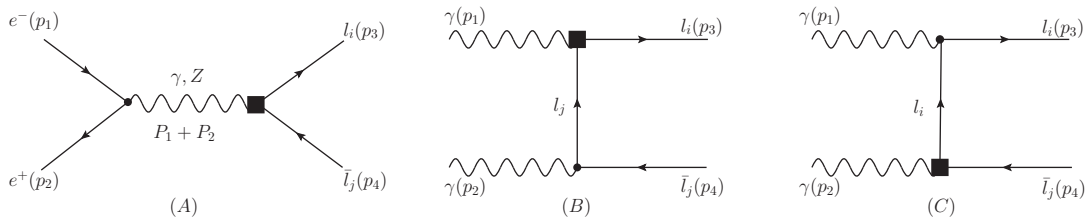

FIG. 2: Feynman diagrams for the production $e^+e^-(\gamma\gamma) \to l_i\bar{l}_j$ in the LHT model with the black squares denoting the effective $\bar{l}_i l_j Z(\gamma)$ vertex introduced in [21]. Diagrams with the two photon lines crossed are not shown for $\gamma\gamma \to l_i\bar{l}_j$.

We use the code LoopTools [22] to calculate the loop functions appeared in the effective vertexes.

B. Amplitudes for $e^+e^-(\gamma\gamma) \to l_i\bar{l}_j$

With the aid of the effective $\bar{l}_i l_j Z(\gamma)$ vertex, one can write down the amplitude of $e^+e^- \to l_i\bar{l}_j$ by a straightforward calculation of Fig. 2(A):

$$M_A = M_A^\gamma + M_A^Z, \tag{7}$$

with

$$\begin{aligned} M_A^\gamma &= -\frac{e}{(p_1+p_2)^2}\bar{u}_{l_i}(p_3)\Gamma^\mu_{\bar{l}_i l_j\gamma}(p_3,p_4)v_{\bar{l}_j}(p_4)\bar{v}_{e^+}(p_2)\gamma_\mu u_{e^-}(p_1), \\ M_A^Z &= \frac{g}{\cos\theta_W}\frac{1}{(p_1+p_2)^2-M_Z^2}\bar{u}_{l_i}(p_3)\Gamma^\mu_{\bar{l}_i l_j Z}(p_3,p_4)v_{\bar{l}_j}(p_4)\bar{v}_{e^+}(p_2)\gamma_\mu \\ &\quad \times[(-\frac{1}{2}+\sin^2\theta_W)P_L + (\sin^2\theta_W)P_R]u_{e^-}(p_1), \end{aligned} \tag{8}$$

where $\Gamma^\mu_{\bar{l}_i l_j Z}$ ($\Gamma^\mu_{\bar{l}_i l_j\gamma}$) is the effective $\bar{l}_i l_j Z(\bar{l}_i l_j\gamma)$ vertex which depends on the lepton momenta p_3 and p_4, $P_L = \frac{1}{2}(1-\gamma_5)$ and $P_R = \frac{1}{2}(1+\gamma_5)$.

Similarly, the amplitude of $\gamma\gamma \to l_i\bar{l}_j$ is given by

$$\begin{aligned} M_B &= \frac{e}{(p_3-p_1)^2-m_{l_j}^2}\bar{u}_{l_i}(p_3)\Gamma^\mu_{\bar{l}_i l_j\gamma}(p_3,p_1-p_3)\epsilon_\mu(p_1)(\not{p}_3-\not{p}_1+m_{\bar{l}_j})\not{\epsilon}(p_2)v_{\bar{l}_j}(p_4), \\ M_C &= \frac{e}{(p_2-p_4)^2-m_{l_i}^2}\bar{u}_{l_i}(p_3)\not{\epsilon}(p_1)(\not{p}_2-\not{p}_4+m_{l_i})\Gamma^\mu_{\bar{l}_i l_j\gamma}(p_2-p_4,p_4)\epsilon_\mu(p_2)v_{\bar{l}_j}(p_4). \end{aligned} \tag{9}$$

For the $\gamma\gamma$ collision at the ILC, the photon beams are generated by the backward Compton scattering of incident electron- and laser-beams just before the interaction point. The events number is obtained by convoluting the cross section with the photon beam luminosity distribution. For $\gamma\gamma$ collider the events number is obtained by

$$N_{\gamma\gamma\to l_i\bar{l}_j} \;=\; \int \mathrm{d}\sqrt{s_{\gamma\gamma}}\frac{\mathrm{d}\mathcal{L}_{\gamma\gamma}}{\mathrm{d}\sqrt{s_{\gamma\gamma}}}\hat{\sigma}_{\gamma\gamma\to l_i\bar{l}_j}(s_{\gamma\gamma}) \equiv \mathcal{L}_{e^+e^-}\;\sigma_{\gamma\gamma\to l_i\bar{l}_j}(s_{e^+e^-}), \tag{10}$$

where $\mathrm{d}\mathcal{L}_{\gamma\gamma}/\mathrm{d}\sqrt{s_{\gamma\gamma}}$ is the photon beam luminosity distribution and $\sigma_{\gamma\gamma\to l_i\bar{l}_j}(s_{e^+e^-})$, with $s_{e^+e^-}$ being the energy-square of e^+e^- collision, is defined as the effective cross section of $\gamma\gamma \to l_i\bar{l}_j$. In optimum case, $\sigma_{\gamma\gamma\to l_i\bar{l}_j}$ can be written as [23]

$$\sigma_{\gamma\gamma\to l_i\bar{l}_j}(s_{e^+e^-}) \;=\; \int_{\sqrt{a}}^{x_{max}} 2z\mathrm{d}z\;\hat{\sigma}_{\gamma\gamma\to l_i\bar{l}_j}(s_{\gamma\gamma}=z^2s_{e^+e^-})\int_{z^2/x_{max}}^{x_{max}}\frac{\mathrm{d}x}{x}\;F_{\gamma/e}(x)\;F_{\gamma/e}(\frac{z^2}{x}), \tag{11}$$

where $F_{\gamma/e}$ denotes the energy spectrum of the back-scattered photon for unpolarized initial electron and laser photon beams given by

$$F_{\gamma/e}(x) \;=\; \frac{1}{D(\xi)}\left(1-x+\frac{1}{1-x}-\frac{4x}{\xi(1-x)}+\frac{4x^2}{\xi^2(1-x)^2}\right). \tag{12}$$

The definitions of parameters ξ, $D(\xi)$ and x_{max} can be found in [23]. In our numerical calculation, we choose $\xi = 4.8$, $D(\xi) = 1.83$ and $x_{max} = 0.83$.

Before we end this section, we emphasize two advantages of $\gamma\gamma$ collision over the e^+e^- collision of the ILC in probing the LFV interaction. One is for the process $e^+e^- \to l_i\bar{l}_j$, it occurs only via s-channel, so its rate is suppressed by the photon propagator and the Z propagator. While for $\gamma\gamma \to l_i\bar{l}_j$, there is no such suppression. The other is the $\gamma\gamma$ collision provides a cleaner environment than the e^+e^- collision, so is well suited to probe new physics.

IV. NUMERICAL RESULTS

In our calculations, we neglect terms proportional to v^2/f^2 in the new gauge boson masses and also in the relevant Feynman rules. We take the SM parameters as [24]:

$$m_e = 0.0051\ \text{GeV}, \qquad m_\mu = 0.106\ \text{GeV}, \qquad m_\tau = 1.777\ \text{GeV},$$
$$m_Z = 91.2\ \text{GeV}, \qquad s_W^2 = 0.231, \qquad \alpha_e = 1/128.8.$$

Among the LHT parameters, we must specify the breaking scale f, the mirror lepton masses as well as the matrix V_{H_l}. We choose $f = 500$ GeV and $f = 1000$ GeV as two representative cases, and as shown in [5], these two cases are consistent with precision electroweak data. About the mirror lepton masses, we fix $m_{l_H^1} = m_{l_H^2} = m_{H12} = 500$ GeV, and vary $m_{l_H^3} \equiv m_{H3}$ in the range of $600 - 1200$ GeV for $f = 500$ GeV and $600 - 1500$ GeV for $f = 1000$ GeV. We set $V_{Hl} = V_{PMNS}$ (or equally $V_{H\nu} = I$), and like [7, 18] did, determine the elements of V_{PMNS} from the neutrino experiments [25–29] with the three Majorana phases in V_{PMNS} taken to be zero. From the results of [18], one can learn that our choice of the LHT parameters satisfies the constraint from $m_{H_i} \leq 4.8f^2$ and the rare decays $l_i \to l_j\gamma$. By the way, in calculating the rates for $\gamma\gamma \to l_i\bar{l}_j$ we require $|\cos\theta_l| < 0.9$ and $p_T^l > 20$ GeV [15].

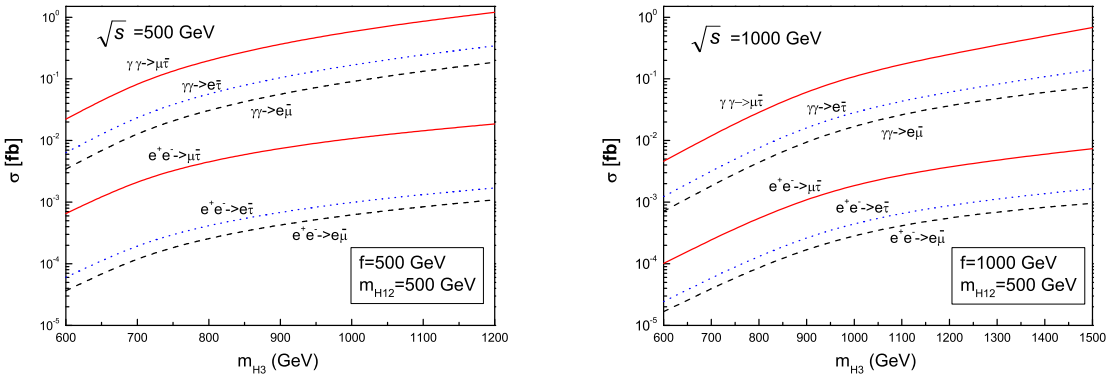

FIG. 3: The production rates for the processes $e^+e^-(\gamma\gamma) \to l_i\bar{l}_j$ as a function of m_{H3}.

Our results are summarized in Fig. 3 with different $l_i\bar{l}_j$ states considered. From this figure, one can get three conclusions. The first is the production rates of $e^+e^-(\gamma\gamma) \to l_i\bar{l}_j$ monotonously increase with m_{H3} becoming larger. This is because these processes proceed in a way quite similar to the GIM mechanism of the SM, so the more significant the mass splitting between the mirror leptons is, the larger the rates become. The second is the rate for $\gamma\gamma \to l_i\bar{l}_j$ is several orders larger than that of $e^+e^- \to l_i\bar{l}_j$. The reason is, as we mentioned before, that the process $e^+e^- \to l_i\bar{l}_j$ is s-channel suppressed, while the process $\gamma\gamma \to l_i\bar{l}_j$ gets contribution from u-channel and t-channel and there is no such suppression. The last is among the LFV processes, the rate for $e\mu$ final state is much

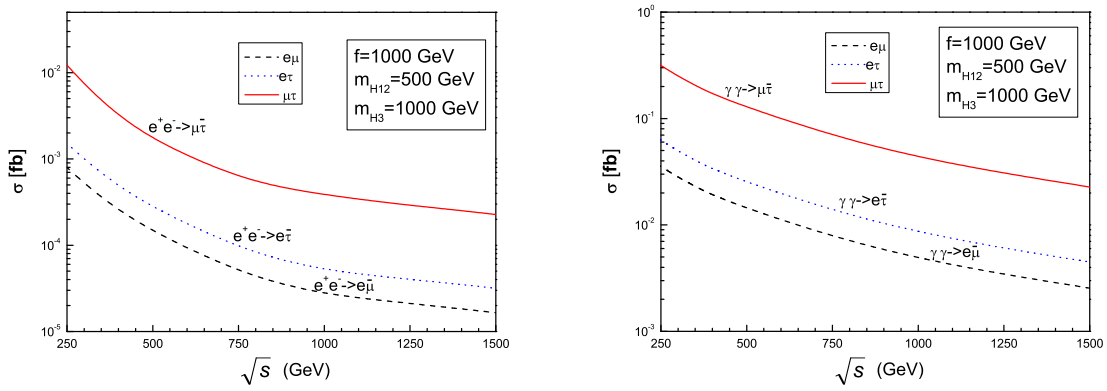

FIG. 4: The production rates for the processes $e^+e^-(\gamma\gamma) \to l_i\bar{l}_j$ as a function of center-of-mass energy $\sqrt{s}$.

smaller than that for $e\tau$ or $\mu\tau$ state. This is because the processes with $e\mu$ final state are stringently constrained by the decay $\mu \to e\gamma$.

Since the production rates for $\gamma\gamma \to e\tau, \mu\tau$ are significantly larger than the other production rates, we now discuss their observability at the ILC. For $\gamma\gamma \to e\tau$, its main backgrounds come from $\gamma\gamma \to \tau^+\tau^- \to \tau^-\nu_e\bar{\nu}_\tau e^+$, $\gamma\gamma \to W^+W^- \to \tau^-\nu_e\bar{\nu}_\tau e^+$ and $\gamma\gamma \to e^+e^-\tau^+\tau^-$. In order to enhance the ratio of the signal to the background, one usually adds the following cuts in Monte Carlo simulation [15]: $|\cos\theta_l| < 0.9$ and $p_T^e > 20$GeV. With these cuts, the rates for the background processes at $\sqrt{s}$= 500GeV are 9.7×10^{-4} fb for $\gamma\gamma \to \tau^+\tau^- \to \tau^-\nu_e\bar{\nu}_\tau e^+$, 1.0×10^{-1} fb for $\gamma\gamma \to W^+W^- \to \tau^-\nu_e\bar{\nu}_\tau e^+$, and 2.4×10^{-2} fb for $\gamma\gamma \to e^+e^-\tau^+\tau^-$ respectively (see Table 1 of [15]). This implies that to get a 3σ observing sensitivity with 3.45×10^{-2} fb^{-1} integrated luminosity [30], the production rate for $\gamma\gamma \to e\bar{\tau}$ must be larger than 2.5×10^{-2} fb [15]. Compared this value with the results in Fig. 3, one can learn that the process $\gamma\gamma \to e\bar{\tau}$ may be observable in broad regions of the LHT parameter space. With regard to $\gamma\gamma \to \mu\bar{\tau}$, since its production rate may be several times larger than that for $\gamma\gamma \to e\bar{\tau}$ while the background rates are same, one can conclude that $\gamma\gamma \to \mu\bar{\tau}$ is more powerful in probing the LHT model.

For the sake of providing more information of the ILC in probing the LHT model, we also show the rates of $e^+e^-(\gamma\gamma) \to l_i\bar{l}_j$ as the function of center-of-mass energy of the ILC $\sqrt{s}$ in Fig. 4. We see that with the increase of $\sqrt{s}$, the production rates become smaller

TABLE I: The theoretical predictions of the rates for $\gamma\gamma \to l_i\bar{l}_j$ at $\sqrt{s} = 500$ GeV in the optimum case of different models.

	MSSM with R-parity	MSSM without R-parity	TC2	LHT
$\gamma\gamma \to \mu\bar{\tau}$	$\mathcal{O}(10^{-2})$[15]	$\mathcal{O}(10^{-2})$[16]	$\mathcal{O}(1)$[17]	$O(1)$
$\gamma\gamma \to e\bar{\tau}$	$\mathcal{O}(10^{-1})$[15]	$\mathcal{O}(10^{-2})$[16]	$\mathcal{O}(1)$[17]	$O(10^{-1})$
$\gamma\gamma \to e\bar{\mu}$	$\mathcal{O}(10^{-3})$ [15]	$\mathcal{O}(10^{-4})$[16]	$\mathcal{O}(10^{-3})$[17]	$O(10^{-1})$

which is similar to the behaviors of the supersymmetric models [15, 16].

We also list the theoretical predictions of the production rates in the optimum case of different models in Table I. From this table, one can learn that, due to enhanced coupling strength, the production rates in the LHT and TC2 model can be significantly larger than that in R-parity violating MSSM. So the processes of $\gamma\gamma \to l_i\bar{l}_j$ may be utilized to distinguish new physics models.

V. CONCLUSION

In the LHT model, the interactions between the mirror leptons and the SM leptons induce the LFV processes at loop level. We study the LFV productions $e^+e^-(\gamma\gamma) \to l_i\bar{l}_j$ at the ILC, and find that, compared with the SM predictions, the production rates in the LHT can be greatly enhanced. In particular, the production rates for $\gamma\gamma \to \mu\bar{\tau}$ and for $\gamma\gamma \to e\bar{\tau}$ can reach 1 fb and 10^{-1} fb respectively in optimum case, which fall within the 3σ observing sensitivity of the ILC. Therefore, these LFV production process at the ILC may be utilized to probe the LHT model.

VI. ACKNOWLEDGMENTS

We would like to thank Junjie Cao for helpful discussions and kindly improving our manuscript. This work is supported by the National Natural Science Foundation of China under Grant Nos.10775039, 11075045, by Specialized Research Fund for the Doctoral Program of Higher Education under Grant No.20094104110001 and by HASTIT under

Grant No.2009HASTIT004.

[1] N. Arkani-Hamed, A. G. Cohen and H. Georgi, *Phys. Lett.* B**513**, 232(2001); N. Arkani-Hamed, et al., *JHEP* **0208**, 020(2002); *JHEP* **0208**, 021(2002); I. Low, W. Skiba and D. Smith, *Phys. Rev.* D**66**, 072001(2002); D. E. Kaplan and M. S chmaltz, *JHEP* **0310**, 039(2003).

[2] N. Arkani-Hamed, A. G. Cohen, E. Katz, A. E. Nelson, *JHEP* **0207**, 034(2002); S. Chang, *JHEP* **0312**, 057(2003); T. Han, H. E. Logan, B. McElrath and L. T. Wang, *Phys. Rev.* D**67**, 095004(2003); M. Schmaltz, D. Tucker-smith, Ann. Rev. Nucl. Part. Sci. **55**, 229(2005).

[3] J. L. Hewett, F. J. Petriello and T. G. Rizzo, *JHEP* **0310**, 062(2003); C. Csaki, J. Hubisz, G. D. Kribs, P. Meade and J. Terning, *Phys. Rev.* D**67**, 115002(2003); ibid, *Phys. Rev.* D**68**, 035009(2003); Mu-Chun Chen and Sally Dawson, *Phys. Rev.* D**70**, 015003(2004); W. Kilian and J. Reuter, *Phys. Rev.* D**70**, 015004(2004); Zhenyu Han and WitoldSkiba, *Phys. Rev.* D**72**, 035005(2005).

[4] I. Low, *JHEP*, **0410**, 067(2004); H. C. Cheng and I. Low, *JHEP*, **0408**, 061(2004); J. Hubisz and P. Meade, *Phys. Rev.* D**71**, 035016(2005); J. Hubisz, S. J. Lee and G. Paz, *JHEP*, **0606**, 041(2006).

[5] J. Hubisz, P. Meade, A. Noble, M. Perelstein, *JHEP* **0601**, 135(2006).

[6] J. Hubisz, S. J. Lee, and G. Paz, *JHEP* **0606**, 041(2006).

[7] See for example, M. Blanke, A. J. Buras, A. Poschenrieder, S. Recksiegel, C. Tarantino, S. Uhlig and A. Weiler, *JHEP* **0701**, 066(2007).

[8] M. Blanke, A. J. Buras, A. Poschenrieder, Recksiegel C. Tarantino, S. Uhlig and A. Weiler, *JHEP* **0611**, 062(2006).

[9] X. L. Wang, Y. J. Zhang, H. L. Jin, Y. H. Xi, *Nucl. Phys.* B**810**, 266(2009); Hou Hong-Sheng, *Phys. Rev.* D**75**, 094010(2007). X. L. Wang, H. L. Jin, Y. J. Zhang, Y. H. Xi, *Nucl. Phys.* B**807**, 210(2009); X. F Han, L. Wang, J. M. Yang, *Phys. Rev.* D**78**, 075017(2008).

[10] G. Bonvicini et al. CLEO Collaboration, *Phys. Rev. Lett.* **79**, 1221(1997); Y. Enari et al., Belle Collaboration, *Phys. Lett.* B**622**, 218(2005); Y. Enari et al., Belle Collaboration, *Phys. Rev. Lett.* **93**, 081803(2004); Y. Yusa et al., Belle Collaboration, *Phys. Lett.* B**589**,

103(2004).

[11] M. L. Brooks, et al., MEGA Collaboration, *Phys. Rev. Lett.* **83**, 1521(1999); B. Aubert, et al., BABAR Collaboration, *Phys. Rev. Lett.* **95**, 041802(2005); K. Hayasaka, et al., Belle Collaboration, *Phys. Lett.* B**666**, 16(2008); M. Ahmed et al. MEGA Collaboration, *Phys. Rev.* D**65**, 112002(2008).

[12] For lepton flavor violation in SUSY, see, e.g., J. Hisano, T. Moroi, K.Tobe, M. Yamaguchi, *Phys. Lett.* B**357**, 579(1995); J. Ellis, *et al.*, *EPJC* **14**, 319(2000); J. L. Feng, Y. Nir, Y. Shadmi, *Phys. Rev.* D**61** 113005(2000); W. Buchmuller, D. Delepine, L. T. Handoko, *Nucl. Phys.* B**576**, 445(2000); J. Sato, K. Tobe, T. Yanagita, *Phys. Lett.* B**498**, 189(2001); M. C. Chen, K. T. Mahanthappa *Phys. Rev.* D**70** 113013(2004); J. Cao, Z. Xiong, J. M. Yang, *EPJC* **32**, 245(2004); D. Atwood, *et al.*, *Phys. Rev.* D**66** 093005(2002); J. I. Illana, M. Masip, *Phys. Rev.* D**67** 035004(2003); Y. B. Sun *et al.*, *JHEP* **0409**, 043(2004).

[13] For lepton flavor violation in TC2, see, e.g., Chong-xing Yue, Hong Li, Yanming Zhang, Yong jia, *Phys. Lett.* B**536**, 67(2002); Chong-xing Yue, Lanjun Liu, Dongqi Yu, *Phys. Rev.* D**68** 035002(2003).

[14] Wang Shao-Ming *et al.*, *Phys.Rev.* D**74** 057902 (2006).

[15] M. Cannoni, C. Carimalo, W. Da Silva and O. Panella, *Phys. Rev.* D**72** 115004(2005).

[16] Junjie Cao, Lei Wu, Jinmin Yang, *Nucl. Phys.* B**829**, 370(2009).

[17] Guo-Li Liu arXiv:1002.0659

[18] M. Blanke, A. J. Buras, B. Duling, A. Poschenrieder and C. Tarantino, *JHEP* **0705**, 013(2007);

[19] S . R. Choudhury et al., *Phys. Rev.* D**75**, 055011(2007);

[20] For lepton flavor violation in LHT, see, e.g., F. del Aguila, J. I. Illana and M. D. Jenkins, *JHEP* **0901**, 080(2009); S . R. Choudhury et al., *Phys. Rev.* D**75**, 055011(2007); A. Goyal arXiv:hep-ph/0609095; Chong-Xing Yue, Jin-Yan Liu and Shi-Hai Zhu, *Phys. Rev.* D**78**, 095006(2007); Naveen Gaur, *AIP Conf. Proc.* **357**, 981(2009); Cecilia Tarantino, *J. Phys. Conf. Ser* **110**, 072043(2008).

[21] J. J. Cao, G. Eilam, M. Frank, K. Hikasa, G. L. Liu, I. Turan, and J. M. Yang, *Phys. Rev.* D**75**, 075021(2007).

[22] T. Hahn, M. Perez-Victoria, *Comput. Phys. Commun.* **118**, 153(1999); T. Hahn, *Nucl.*

Phys. Proc. Suppl. **135**, 333(2004).

[23] I. F. Ginzburg *et al.*, *Nucl. Instrum.* 219, 5(1984); V. I. Telnov, *Nucl. Instrum. Meth.* 294, 72(1990).

[24] C. Amsler *et al.*, Particle Data Group, *Phys. Lett.* B**667**, 1(2008).

[25] O. Mena, S. J. Parke, *Phys. Rev* D**69** 117301(2004).

[26] R. N. Mohapatra *et al.*, *Phys. Rev.* D**69** 117301(2004), hep-ph/0510213.

[27] C. Giunti, hep-ph/0611125.

[28] J. D. Bjorken, P. F. Harrison, W. G. Scott, *Phys. Rev.* D**74** 073012(2006).

[29] G. Ahuja, M. Gupta, M. Randhawa, hep-ph/0611324.

[30] B. Badelek *et al.*, *Int. J. Mod. Phys.* A**19**, 5097(2004).

Appendix A: Explicit expressions of $\Gamma^{\mu}_{\bar{e}\mu\gamma}$ and $\Gamma^{\mu}_{\bar{e}\mu Z}$

In this appendix, we list the explicit expressions for the effective $\bar{e}\mu\gamma$ ($\bar{e}\mu Z$) vertex $\Gamma^{\mu}_{\bar{e}\mu\gamma}(\Gamma^{\mu}_{\bar{e}\mu Z})$. These expressions are obtained by a straightforward calculation of Fig. 1. In our calculation, we neglect terms proportional to v^2/f^2, which appear in the new gauge boson masses and also in the relevant Feynman rules. Other effective vertices such as $\bar{e}\tau(\bar{\mu}\tau)\gamma$ and $\bar{e}\tau(\bar{\mu}\tau)Z$ can be obtained in a similar way.

$$
\begin{aligned}
\Gamma^{\mu}_{\bar{e}\mu\gamma}(p_e,p_{\bar{\mu}}) &= \Gamma^{\mu}_{\bar{e}\mu\gamma}(\eta)+\Gamma^{\mu}_{\bar{e}\mu\gamma}(\omega^0)+\Gamma^{\mu}_{\bar{e}\mu\gamma}(\omega^{\pm})+\Gamma^{\mu}_{\bar{e}\mu\gamma}(A_H)+\Gamma^{\mu}_{\bar{e}\mu\gamma}(Z_H)+\Gamma^{\mu}_{\bar{e}\mu\gamma}(W_H^{\pm})\\
&\quad +\Gamma^{\mu}_{\bar{e}\mu\gamma}(W_H^{\pm}\omega^{\pm}),\\
\Gamma^{\mu}_{\bar{e}\mu\gamma}(\eta) &= -\frac{i}{16\pi^2}\frac{eg'^2}{100M^2_{A_H}}(V_{Hl})^*_{ie}(V_{Hl})_{i\mu}(A+B+C)\\
A &= \{\frac{1}{p_e^2-m_\mu^2}[m^2_{Hi}(m_\mu^2B_0^a+p_e^2B_1^a)\gamma^\mu P_L+m_em_\mu(m^2_{Hi}B_0^a+p_e^2B_1^a)\gamma^\mu P_R\\
&\quad +m_e(m^2_{Hi}B_0^a+m_\mu^2B_1^a)\not{p}_e\gamma^\mu P_L+m^2_{Hi}m_\mu(B_0^a+B_1^a)\not{p}_e\gamma^\mu P_R]\}\\
B &= \{\frac{1}{p_{\bar{\mu}}^2-m_e^2}[m^2_{Hi}(m_e^2B_0^b+p_{\bar{\mu}}^2B_1^b)\gamma^\mu P_L+m_em_\mu(m^2_{Hi}B_0^b+p_{\bar{\mu}}^2B_1^b)\gamma^\mu P_R\\
&\quad -m_em^2_{Hi}(B_0^b+B_1^b)\gamma^\mu\not{p}_{\bar{\mu}}P_L-m_\mu(m^2_{Hi}B_0^b+m_e^2B_1^b)\not{p}_{\bar{\mu}}\gamma^\mu P_R]\}\\
C &= \{[-m^4_{Hi}C_0^1\gamma^\mu P_L-m_em_\mu m^2_{Hi}C_0^1\gamma^\mu P_R+m^2_{Hi}m_eC_\alpha^1\gamma^\alpha\gamma^\mu P_L\\
&\quad +m_em^2_{Hi}(-\gamma^\mu\not{p}_eC_0^1-\gamma^\mu\not{p}_{\bar{\mu}}C_0^1+\gamma^\mu\gamma^\alpha C_\alpha^1)P_L+m^2_{Hi}m_\mu C_\alpha^1\gamma^\alpha\gamma^\mu P_R\\
&\quad +m^2_{Hi}m_\mu(\gamma^\mu\gamma^\alpha C_\alpha^1-\gamma^\mu\not{p}_eC_0^1-\gamma^\mu\not{p}_{\bar{\mu}}C_0^1)P_R+m^2_{Hi}(\gamma^\alpha\gamma^\mu\not{p}_eC_\alpha^1+\gamma^\alpha\gamma^\mu\not{p}_{\bar{\mu}}C_\alpha^1\\
&\quad -\gamma^\alpha\gamma^\mu\gamma^\beta C_{\alpha\beta}^1)P_L+m_em_\mu(\gamma^\alpha\gamma^\mu\not{p}_eC_\alpha^1+\gamma^\alpha\gamma^\mu\not{p}_{\bar{\mu}}C_\alpha^1-\gamma^\alpha\gamma^\mu\gamma^\beta C_{\alpha\beta}^1)P_R]\},\\
\Gamma^{\mu}_{\bar{e}\mu\gamma}(\omega^0) &= -\frac{i}{16\pi^2}\frac{eg^2}{4M^2_{Z_H}}(V_{Hl})^*_{ie}(V_{Hl})_{i\mu}(D+E+F)\\
D &= A(B_0^a\to\ B_0^c,B_1^a\to\ B_1^c)\\
E &= B(B_0^b\to\ B_0^d,B_1^b\to\ B_1^d)\\
F &= C(C_{\alpha\beta}^1\to\ C_{\alpha\beta}^2,C_\alpha^1\to\ C_\alpha^2,C_0^1\to\ C_0^2),\\
\Gamma^{\mu}_{\bar{e}\mu\gamma}(\omega^{\pm}) &= -\frac{i}{16\pi^2}\frac{eg^2}{2M^2_{W_H}}(V_{Hl})^*_{ie}(V_{Hl})_{i\mu}[G+H-J]\\
J &= \{m^2_{Hi}m_e(p_e^\mu C_0^4+p_{\bar{\mu}}^\mu C_0^4+2C_\mu^4)P_L+m^2_{Hi}m_\mu(p_e^\mu C_0^4+p_{\bar{\mu}}^\mu C_0^4+2C_\mu^4)P_R\\
&\quad -m^2_{Hi}[p_{\mu\alpha}(p_e^\mu+p_{\bar{\mu}}^\mu+2C_\mu^4)+(p_e^\mu+p_{\bar{\mu}}^\mu)C_\alpha^4+2C_{\mu\alpha}^4]\gamma^\alpha P_L\\
&\quad -m_em_\mu[p_{e\alpha}(p_e^\mu+p_{\bar{\mu}}^\mu+2C_\mu^4)+(p_e^\mu+p_{\bar{\mu}}^\mu)C_\alpha^4+2C_{\mu\alpha}^4]\gamma^\alpha P_L\}
\end{aligned}
$$

$$G = A(B_0^a \to \ B_0^e, B_1^a \to \ B_1^e)$$

$$H = B(B_0^b \to \ B_0^f, B_1^b \to \ B_1^f),$$

$$\Gamma^{\mu}_{\bar{e}\mu\gamma}(A_H) = -\frac{i}{16\pi^2}\frac{eg'^2}{50}(V_{Hl})^*_{ie}(V_{Hl})_{i\mu}(K+L+M)$$

$$K = \frac{1}{p_e^2 - m_\mu^2}[p_e^2 B_1^a + m_\mu \not{p}_e B_1^a]\gamma^\mu P_L$$

$$L = \frac{1}{p_{\bar{\mu}}^2 - m_e^2}[p_{\bar{\mu}}^2 B_1^b - m_e \not{p}_{\bar{\mu}} B_1^b]\gamma^\mu P_L$$

$$M = [(\not{p}_e + \not{p}_{\bar{\mu}})C_\alpha^1 \gamma^\mu \gamma^\alpha - m_{Hi}^2 C_0^1 \gamma^\mu - C_{\alpha\beta}^1 \gamma^\alpha \gamma^\mu \gamma^\beta]P_L,$$

$$\Gamma^{\mu}_{\bar{e}\mu\gamma}(Z_H) = -\frac{i}{16\pi^2}\frac{eg^2}{2}(V_{Hl})^*_{ie}(V_{Hl})_{i\mu}(N+O+P)$$

$$N = K(B_1^a \to \ B_1^c)$$

$$O = L(B_1^b \to \ B_1^d)$$

$$P = M(C_{\alpha\beta}^1 \to \ C_{\alpha\beta}^2, C_\alpha^1 \to \ C_\alpha^2, C_0^1 \to \ C_0^2),$$

$$\Gamma^{\mu}_{\bar{e}\mu\gamma}(W_H^\pm) = -\frac{i}{16\pi^2}\frac{eg^2}{2}(V_{Hl})^*_{ie}(V_{Hl})_{i\mu}(2Q+2R-T)$$

$$T = [(p_e^2 + 2B_0^f + 2m_{WH}^2 C_0^4)\gamma^\mu P_L + (4C_{\alpha\mu}^4 + 2C_\alpha^4 p_b^\mu + 2C_\alpha^4 p_{\bar{\mu}}^\mu)\gamma^\alpha P_L + 2\not{p}_e(C_\mu^4$$
$$+\not{p}_e p_{\bar{\mu}}^b C_0^4 + p_{\bar{\mu}}^\mu C_0^4)P_L + (2C_\alpha^4 \not{p}_e \gamma^\alpha + C_\alpha^4 \gamma^\alpha \not{p}_e + 2C_\alpha^4 \not{p}_{\bar{\mu}} \gamma^\alpha + 2\not{p}_{\bar{\mu}}\not{p}_e C_0^4)\gamma^\mu P_L]$$

$$Q = K(B_1^a \to \ B_1^e)$$

$$R = L(B_1^b \to \ B_1^f),$$

$$\Gamma^{\mu}_{\bar{e}\mu\gamma}(W_H^\pm \omega^\pm) = \frac{i}{16\pi^2}\frac{g^2 e}{2}(V_{Hl})^*_{ie}(V_{Hl})_{i\mu}$$
$$\times[m_\mu(\gamma^\mu \not{p}_e C_0^4 + \gamma^\mu \gamma^\alpha C_\alpha^4)P_R + m_e(\gamma^\mu \not{p}_e C_0^4 + \gamma^\mu \gamma^\alpha C_\alpha^4)P_L].$$

$$\Gamma^{\mu}_{\bar{e}\mu Z}(p_e, p_{\bar{\mu}}) = \Gamma^{\mu}_{\bar{e}\mu Z}(\eta) + \Gamma^{\mu}_{\bar{e}\mu Z}(\omega^0) + \Gamma^{\mu}_{\bar{e}\mu Z}(\omega^\pm) + \Gamma^{\mu}_{\bar{e}\mu Z}(A_H) + \Gamma^{\mu}_{\bar{e}\mu Z}(Z_H) + \Gamma^{\mu}_{\bar{e}\mu Z}(W_H^\pm)$$
$$+\Gamma^{\mu}_{\bar{e}\mu Z}(W_H^\pm \omega^\pm),$$

$$\Gamma^{\mu}_{\bar{e}\mu Z}(\eta) = \frac{i}{16\pi^2}\frac{g}{\cos\theta_W}(-\frac{1}{2} + \sin^2\theta_W)\frac{g'^2}{100 M_{A_H}^2}(V_{Hl})^*_{ie}(V_{Hl})_{i\mu}(A' + B' + C')$$

$$A' = \{\frac{1}{p_e^2 - m_\mu^2}[(-\frac{1}{2} + \sin^2\theta_W)(m_{Hi}^2 m_\mu^2 B_0^a + m_{Hi}^2 p_e^2 B_1^a)\gamma^\mu P_L$$
$$+\sin^2\theta_W m_e m_\mu (m_{Hi}^2 B_0^a + p_e^2 B_1^a)\gamma^\mu P_R + (-\frac{1}{2} + \sin^2\theta_W)(m_e m_{Hi}^2 B_0^a$$
$$+m_e m_\mu^2 B_1^a)\not{p}_e \gamma^\mu P_L + \sin^2\theta_W m_{Hi}^2 m_\mu (B_0^a + B_1^a)\not{p}_e \gamma^\mu P_R]\}$$

$$B' = \{\frac{1}{p_{\bar{\mu}}^2 - m_e^2}[(-\frac{1}{2} + \sin^2\theta_W)(m_{Hi}^2 m_e^2 B_0^b + m_{Hi}^2 p_{\bar{\mu}}^2 B_1^b)\gamma^\mu P_L$$
$$+\sin^2\theta_W m_e m_\mu (m_{Hi}^2 B_0^b + p_{\bar{\mu}}^2 B_1^b)\gamma^\mu P_R - \sin^2\theta_W m_e m_{Hi}^2 (B_0^b$$
$$+B_1^b)\gamma^\mu \not{p}_{\bar{\mu}} P_L - (-\frac{1}{2} + \sin^2\theta_W) m_\mu (m_{Hi}^2 B_0^b + m_e^2 B_1^b)\not{p}_{\bar{\mu}} \gamma^\mu P_R]\}$$

$$C' = (-\frac{1}{2} + \sin^2\theta_W)C,$$

$$\Gamma^{\mu}_{\bar{e}\mu Z}(\omega^0) = \frac{i}{16\pi^2}\frac{g}{\cos\theta_W}\frac{g^2}{4M^2_{Z_H}}(V_{Hl})^*_{ie}(V_{Hl})_{i\mu}m^2_{Hi}(D' + E' + F')$$

$$D' = A'(B^a_0 \to \ B^c_0, B^a_1 \to \ B^c_1)$$

$$E' = B'(B^b_0 \to \ B^d_0, B^b_1 \to \ B^d_1)$$

$$F' = C'(C^1_{\alpha\beta} \to \ C^2_{\alpha\beta}, C^1_{\alpha} \to \ C^2_{\alpha}, C^1_0 \to \ C^2_0),$$

$$\Gamma^{\mu}_{\bar{e}\mu Z}(\omega^{\pm}) = \frac{i}{16\pi^2}\frac{g}{\cos\theta_W}\frac{g^2}{2M^2_{W_H}}(V_{Hl})^*_{ie}(V_{Hl})_{i\mu}(G' + H' + I' + J')$$

$$G' = A'(B^a_0 \to \ B^e_0, B^a_1 \to \ B^e_1)$$

$$H' = B'(B^b_0 \to \ B^f_0, B^b_1 \to \ B^f_1)$$

$$I' = (C'(C^1_{\alpha\beta} \to C^3_{\alpha\beta}, C^1_{\alpha} \to \ C^3_{\alpha}, C^1_0 \to \ C^3_0)$$

$$J' = \cos^2\theta_W J,$$

$$\Gamma^{\mu}_{\bar{e}\mu Z}(A_H) = \frac{i}{16\pi^2}\frac{g}{\cos\theta_W}\frac{g'^2}{50}(V_{Hl})^*_{ie}(V_{Hl})_{i\mu}(K' + L' + M')$$

$$K' = \frac{1}{p^2_e - m^2_{\mu}}[(-\frac{1}{2} + \sin^2\theta_W)p^2_e B^a_1 + \sin^2\theta_W m_{\mu}\not{p}_e B^a_1]\gamma^{\mu}P_L$$

$$L' = \frac{1}{p^2_{\bar{\mu}} - m^2_e}[(-\frac{1}{2} + \sin^2\theta_W)p^2_{\bar{\mu}} B^b_1 - \sin^2\theta_W m_e\not{p}_{\bar{\mu}} B^b_1]\gamma^{\mu}P_L$$

$$M' = (-\frac{1}{2} + \sin^2\theta_W)[(\not{p}_e + \not{p}_{\bar{\mu}})C^1_{\alpha}\gamma^{\mu}\gamma^{\alpha} - m^2_{Hi}C^1_0\gamma^{\mu} - C^1_{\alpha\beta}\gamma^{\alpha}\gamma^{\mu}\gamma^{\beta}]P_L,$$

$$\Gamma^{\mu}_{\bar{e}\mu Z}(Z_H) = \frac{i}{16\pi^2}\frac{g}{\cos\theta_W}\frac{g^2}{2}(V_{Hl})^*_{ie}(V_{Hl})_{i\mu}(N' + O' + P')$$

$$N' = K'(B^a_1 \to \ B^c_1)$$

$$O' = L'(B^b_1 \to \ B^d_1)$$

$$P' = M'(C^1_{\alpha\beta} \to \ C^2_{\alpha\beta}, C^1_{\alpha} \to \ C^2_{\alpha}, C^1_0 \to \ C^2_0),$$

$$\Gamma^{\mu}_{\bar{e}\mu Z}(W^{\pm}_H) = \frac{i}{16\pi^2}\frac{g}{\cos\theta_W}g^2(V_{Hl})^*_{ie}(V_{Hl})_{i\mu}(Q' + R' + S' + T')$$

$$Q' = K'(B^a_1 \to \ B^e_1)$$

$$R' = L'(B^b_1 \to \ B^f_1)$$

$$S' = -\frac{1}{2}M(C^1_{\alpha\beta} \to \ C^3_{\alpha\beta}, C^1_{\alpha} \to \ C^3_{\alpha}, C^1_0 \to \ C^3_0)$$

$$T' = \cos^2\theta_W T,$$

$$\Gamma^{\mu}_{\bar{e}\mu Z}(W^{\pm}_H\omega^{\pm}) = \frac{i}{16\pi^2}2g^3\cos\theta_W(V_{Hl})^*_{ie}(V_{Hl})_{i\mu}$$
$$\times[m_{\mu}(\gamma^{\mu}\not{p}_e C^4_0 + \gamma^{\mu}\gamma^{\alpha}C^4_{\alpha})P_R + m_e(\gamma^{\mu}\not{p}_e C^4_0 + \gamma^{\mu}\gamma^{\alpha}C^4_{\alpha})P_L].$$

For the two-point and three-point standard loop functions $B_0, B_1, C_0,\ C_{ij}$ in the above expressions are defined as

$$
\begin{aligned}
&C_{ij}^1 = C_{ij}^1(-p_e, -p_{\bar{\mu}}, m_{Hi}, M_{A_H}, m_{Hi}), C_{ij}^2 = C_{ij}^2(-p_e, -p_{\bar{\mu}}, m_{Hi}, M_{Z_H}, m_{Hi}),\\
&C_{ij}^3 = C_{ij}^3(-p_e, -p_{\bar{\mu}}, m_{Hi}, M_{W_H}, m_{Hi}), C_{ij}^4 = C_{ij}^4(p_e, p_{\bar{\mu}}, M_{W_H}, m_{Hi}, M_{W_H}),\\
&B^a = B^a(-p_e, m_{Hi}, M_{A_H}), B^b = B^b(p_{\bar{\mu}}, M_{Hi}, M_{A_H}),\\
&B^c = B^c(-p_e, m_{Hi}, M_{Z_H}), B^d = B^d(p_{\bar{\mu}}, M_{Hi}, M_{Z_H}),\\
&B^e = B^e(-p_e, m_{Hi}, M_{W_H}), B^f = B^f(p_{\bar{\mu}}, M_{Hi}, M_{W_H}).
\end{aligned}
$$